Journal of Biomechanics 86 (2019) 8–16

Contents lists available at ScienceDirect

Journal of Biomechanics

journal homepage: www.elsevier.com/locate/jbiomech
www.JBiomech.com

Direct and indirect effects of joint torque inputs during an induced speed analysis of a swinging motion

Sekiya Koike [a,*], Tatsuya Ishikawa [b], Alexander P. Willmott [c], Neil E. Bezodis [d]

[a] Faculty of Health and Sport Sciences, University of Tsukuba, Japan
[b] Institute of Sport Science, Asics Corporation, Japan
[c] School of Sport and Exercise Science, University of Lincoln, UK
[d] Applied Sports, Technology, Exercise and Medicine Research Centre, Swansea University, UK

ARTICLE INFO

Article history:
Accepted 16 January 2019

Keywords:
Kinetic chain
Whip-like effect
Dynamic contribution
Cause-and-effect relationship
Rugby kicking

ABSTRACT

This study proposed a method to quantify direct and indirect effects of the joint torque inputs in the speed-generating mechanism of a swinging motion. Linear and angular accelerations of all segments within a multi-linked system can be expressed as the sum of contributions from a joint torque term, gravitational force term and motion-dependent term (MDT), where the MDT is a nonlinear term consisting of centrifugal force, Coriolis force and gyroscopic effect moment components. Direct effects result from angular accelerations induced by a joint torque at a given instant, whereas indirect effects arise through the MDT induced by joint torques exerted in the past. These two effects were quantified for the kicking-side leg during a rugby place kick. The MDT was the largest contributor to the foot centre of gravity (CG)'s speed at ball contact. Of the factors responsible for generating the MDT, the direct and indirect effects of the hip flexion-extension torque during both the flight phase (from the final kicking foot take-off to support foot contact) and the subsequent support phase (from support foot contact to ball contact) were important contributors to the foot CG's speed at ball contact. The indirect effect of the ankle plantar-dorsal flexion torque and the direct effect of the knee flexion-extension torque during the support phase showed the largest positive and negative contributions to the foot CG's speed at ball contact, respectively. The proposed method allows the identification of which individual joint torque axes are crucial and the timings of joint torque exertion that are used to generate a high speed of the distal point of a multi-linked system.

1. Introduction

Quantification of the kinetics underpinning the generation of high distal-point speed in swinging motions has provided knowledge regarding how players exert joint torques to produce distinctive patterns of motion within a multi-linked system. Numerous studies have analysed high-speed swinging motions such as baseball pitching (e.g. Feltner and Dapena, 1986; Feltner, 1989; Fleisig et al., 1995; Fleisig et al., 1996a; Fleisig et al., 1996b), tennis serving (e.g. Elliott et al., 2003; Reid et al., 2007), and soccer kicking (e.g. Lees and Rahnama, 2013; Nunome et al., 2002). Although these studies reveal how players exert joint torques during these motions, it remains unclear exactly how and when the individual joint torques exerted affect the speed of the multi-linked system at ball release or ball contact, because such kinetic analyses have limitations in dealing with the cause-and-effect relationship between joint torque inputs and motion outputs.

Since the human body consists of numerous segments connected via joints which are typically assumed to move with only rotational displacements, human movements are performed through angular displacements at joints to achieve coordinated multiple segment motion. The equation of motion for a multi-linked system (e.g. human body) can be expressed generally in the following form (e.g. Kepple et al., 1997; Koike et al., 2017; Zajac et al., 2002) when ignoring modelling errors:

$$\begin{aligned}&(\text{Linear and angular accelerations of all segments}) \text{ or}\\ &\quad(\text{Angular accelerations of all joints}) = (\text{Joint torque term})\\ &\quad+(\text{Gravitational term})+(\text{Motion-dependent term}),\end{aligned} \tag{1}$$

where the motion-dependent term (MDT) is a nonlinear term consisting of centrifugal forces, Coriolis forces and gyroscopic effect moments. Eq. (1) indicates that segmental motion (i.e. linear and

* Corresponding author at: Faculty of Health and Sport Sciences, University of Tsukuba, 1-1-1 Tennodai, Tsukuba City, Ibaraki Prefecture 305-8574, Japan.
E-mail address: koike.sekiya.fp@u.tsukuba.ac.jp (S. Koike).

https://doi.org/10.1016/j.jbiomech.2019.01.032
0021-9290/

Nomenclature

$\boldsymbol{V}$	generalised velocity vector consisting of linear and angular velocity vectors for all the segments
$\dot{\boldsymbol{V}}$	generalised acceleration vector
$\boldsymbol{A}_{\boldsymbol{V},\boldsymbol{T}\mathrm{a}}$	coefficient matrix for the joint torque vector
$\boldsymbol{T}_{\mathrm{a}}$	joint torque vector consisting of active torques
$\bar{\boldsymbol{A}}_{\boldsymbol{V},\mathrm{MDT}}(\boldsymbol{V})$	coefficient matrix for the motion-dependent term, which is a function of the generalised velocity vector
$\boldsymbol{A}_{\boldsymbol{V},\boldsymbol{G}}$	coefficient matrix for gravitational force
$\boldsymbol{G}$	gravitational force vector
$\boldsymbol{B}_{\boldsymbol{V},\mathrm{other}}$	vector consisting of the hip-joint acceleration, segment length fluctuation, and constraint joint axial angle fluctuation terms
$\boldsymbol{A}_{\boldsymbol{V},\mathrm{Hip}}$	coefficient matrix for the hip joint acceleration vector
$\ddot{\boldsymbol{x}}_{\mathrm{Hip}}$	hip joint acceleration
$\boldsymbol{A}_{\boldsymbol{V},\boldsymbol{\eta}}$	coefficient matrix for the double derivation of segment length fluctuation vector
$\boldsymbol{\eta}$	vector of segment length fluctuation
$\boldsymbol{A}_{\boldsymbol{V},\boldsymbol{\varphi}}$	coefficient matrix for the double derivation of constraint joint axial angle fluctuation
$\boldsymbol{\varphi}$	vector of constraint joint axial angle fluctuation
$\dot{\boldsymbol{V}}_{\mathrm{Dir}}$	generalised acceleration vector due to the direct effect of joint torque, gravity and other inputs
$\dot{\boldsymbol{V}}_{\mathrm{Indir}}$	generalised acceleration vector due to the indirect effect of joint torque, gravity and other inputs
k	k-th time instant in the discrete-time system
h	any given instant in time between swing start to time k
Δt	time interval in the discrete-time system
$\boldsymbol{\Psi}_{\boldsymbol{V}}$	coefficient matrix for the generalised velocity vector defined as $\boldsymbol{E}_{18}+\Delta t\bar{\boldsymbol{A}}_{\boldsymbol{V},\mathrm{MDT}}(\boldsymbol{V})$
$\boldsymbol{E}_{18}$	unit matrix with eighteen rows and columns
$\tilde{\boldsymbol{V}}$	measured generalised velocity vector
$\tilde{\boldsymbol{\Psi}}_{\boldsymbol{V}}$	coefficient matrix for the generalised velocity vector defined as $\boldsymbol{E}_{18}+\Delta t\bar{\boldsymbol{A}}_{\boldsymbol{V},\mathrm{MDT}}(\tilde{\boldsymbol{V}})$
$\boldsymbol{V}(0)$	initial value of the generalised velocity vector
i	subscript expressing segment number (i.e. i = 1, thigh; i = 2, shank; i = 3, foot)
$\boldsymbol{S}_i$	selective matrix extracting the linear velocity vector of segment i from the generalised velocity vector
$\dot{\boldsymbol{x}}_i$	linear velocity vector for the centre of gravity of segment i
$\boldsymbol{e}_i$	unit vector for the linear velocity vector for the centre of gravity of segment i
s_{Dir}	speed of segment's centre of gravity induced by direct effect of joint torque inputs
s_{Indir}	speed of segment's centre of gravity induced by indirect effect of joint torque inputs
s_i	contribution to the speed of segment i's centre of gravity induced by both direct and indirect effects of joint torque inputs

angular accelerations) is induced not only by the joint torque inputs and gravitational force but also by the MDT. Motion can be induced by the joint forces exerted at individual joints through motion-dependent mechanisms, even when the inputted joint torques are small. These joint forces do not appear directly as a separate term in Eq. (1) because they are not a primary source like joint torques or gravity but are a secondary source included in the motion-dependent effects arising from the primary sources.

The MDT plays a crucial role in the generation of angular accelerations that influence distal-point speed in high-speed swinging motions (Hirashima, 2008; Hirashima et al., 2008; Koike and Harada, 2014; Koike and Mimura, 2016a, 2016b; Naito and Maruyama, 2008; Naito et al., 2017; Putnam, 1991). Since the MDT is caused by product sums of angular velocities of individual segments, the MDT contribution will be relatively large when angular velocities of several segments increase before ball release or ball contact. The angular velocities of individual segments, caused by earlier joint torques, produce centrifugal and Coriolis forces, and thus the entire joint torque time-histories must be considered when investigating the MDT. At any given instant, previously applied joint torques can still exert an indirect effect on system behaviour through a mechanism sometimes called the "cumulative effect" of joint torque inputs (Zajac et al., 2003; Hirashima et al., 2008; Hirashima, 2008) or "whip-like effect" (Atwater, 1979; Feltner, 1989; Fleisig et al., 1996; Kibler, 1995; Kindall, 1992; Putnam, 1991). However, the contributions of these indirect effects to the generation of segmental speeds have not previously been quantified during any swinging motions. In place of quantifying these indirect effects of joint torque inputs, an analysis decomposing the MDT into kinematic sources (Hirashima et al., 2008; Naito et al., 2010; Naito et al., 2017) has been implemented to explain how the components generate speed. However, this analysis does not reveal which axis of each joint torque is crucial, or the time(s) at which a given joint torque is effective in contributing to the generation of a high distal-point speed. Greater understanding of how each joint torque contributes to speed generation through these indirect effects is still needed. A conversion algorithm that quantifies the generating factors of the MDT has been introduced briefly (Koike and Harada, 2014), but without detailed methods, and was applied to high-speed swinging motions including the tennis serve (Koike and Harada, 2014), baseball batting (Koike and Mimura, 2016b), rugby place kicking (Koike and Bezodis, 2017), and baseball pitching (Koike et al., 2018). Although the factors contributing to the generation of the distal-point speed were examined for these motions, the direct and indirect effects of the joint torque inputs were not separately quantified.

The objectives of this study were to: (1) propose and describe a method which separately quantifies the direct and indirect effects of joint torques to the generation of distal-point speed in a multi-linked system; and (2) illustrate how the direct and indirect contributions differ in an example high-speed swinging motion: a rugby place kick.

2. Methods

2.1. Equation of motion for a multi-linked system

Since the equation of motion for a multi-linked system includes a cause-and-effect relationship between joint torque inputs and motion outputs, the general equation of motion (Eq. (1)) was used to derive a recurrence formula which can take the indirect effect of joint torque inputs into account. The proposed method was applied to the kicking-side lower limb segments during a rugby place kick.

The dynamical equation for the kicking-side leg, consisting of thigh, shank and foot segments, can be expressed as follows (see Appendix 1 for details):

$$\dot{\boldsymbol{V}}=\boldsymbol{A}_{\boldsymbol{V},\boldsymbol{T}\mathrm{a}}\boldsymbol{T}_{\mathrm{a}}+\bar{\boldsymbol{A}}_{\boldsymbol{V},\mathrm{MDT}}(\boldsymbol{V})\boldsymbol{V}+\boldsymbol{A}_{\boldsymbol{V},\boldsymbol{G}}\boldsymbol{G}+\boldsymbol{B}_{\boldsymbol{V},\mathrm{other}} \tag{2}$$

where the vector $\boldsymbol{V}$ denotes the generalised velocity vector $\boldsymbol{V}=\left[\dot{\boldsymbol{x}}_1^{\mathrm{T}}\ \boldsymbol{\omega}_1^{\mathrm{T}}\ \dot{\boldsymbol{x}}_2^{\mathrm{T}}\ \boldsymbol{\omega}_2^{\mathrm{T}}\ \dot{\boldsymbol{x}}_3^{\mathrm{T}}\ \boldsymbol{\omega}_3^{\mathrm{T}}\right]^{\mathrm{T}}$, which consists of the linear velocity

vector $\dot{\boldsymbol{x}}_i$ and angular velocity vector $\boldsymbol{\omega}_i$ of all segments (where subscript i denotes segment number: $i = 1$, thigh; $i = 2$, shank; $i = 3$, foot). The terms on the right-hand-side of Eq. (2) represent the respective contributions to the generation of the generalised velocity vector of the joint torque term, motion-dependent term, gravitational term, and a term consisting of all the remaining sources with the matrices $\boldsymbol{A}_{\boldsymbol{V},\boldsymbol{Ta}}$ and $\boldsymbol{A}_{\boldsymbol{V},\boldsymbol{G}}$ indicating the coefficient matrices for the joint torque vector $\boldsymbol{T}_a$ and gravitational force vector $\boldsymbol{G}$, $\bar{\boldsymbol{A}}_{\boldsymbol{V},\mathrm{MDT}}(\boldsymbol{V})$ being the coefficient matrix associated with the MDT and $\boldsymbol{B}_{\boldsymbol{V},\mathrm{other}}$ indicating the vector consisting of the remaining terms:

$$\boldsymbol{B}_{\boldsymbol{V},\mathrm{other}} = \boldsymbol{A}_{\boldsymbol{V},\mathrm{Hip}}\ddot{\boldsymbol{x}}_{\mathrm{Hip}} + \boldsymbol{A}_{\boldsymbol{V},\boldsymbol{\eta}}\ddot{\boldsymbol{\eta}} + \boldsymbol{A}_{\boldsymbol{V},\varphi}\ddot{\boldsymbol{\varphi}} \tag{3}$$

where the matrix $\boldsymbol{A}_{\boldsymbol{V},\mathrm{Hip}}$ is the coefficient matrix for hip joint acceleration $\ddot{\boldsymbol{x}}_{\mathrm{Hip}}$, the matrices $\boldsymbol{A}_{\boldsymbol{V},\boldsymbol{\eta}}$ and $\boldsymbol{A}_{\boldsymbol{V},\varphi}$ are coefficient matrices for the vectors $\ddot{\boldsymbol{\eta}}$ and $\ddot{\boldsymbol{\varphi}}$, respectively (see Appendix 1 for more detail). These three terms on the right-hand side correspond to the hip joint acceleration, segment length fluctuation and anatomical constraint joint axial angle fluctuation terms, respectively.

Similarly to the combination of "instantaneous and cumulative acceleration vectors" in previous studies (Hirashima et al., 2008; Zajac et al, 2003), the generalised acceleration vector $\dot{\boldsymbol{V}}$ can be expressed as the sum of two types of acceleration vector:

$$\dot{\boldsymbol{V}} = \dot{\boldsymbol{V}}_{\mathrm{Dir}} + \dot{\boldsymbol{V}}_{\mathrm{Indir}}, \tag{4}$$

where $\dot{\boldsymbol{V}}_{\mathrm{Dir}}$ denotes the acceleration vector due to the direct effect of joint torque, gravity and other inputs:

$$\dot{\boldsymbol{V}}_{\mathrm{Dir}} = \boldsymbol{A}_{\boldsymbol{V},\boldsymbol{T}a}\boldsymbol{T}_a + \boldsymbol{A}_{\boldsymbol{V},\boldsymbol{G}}\boldsymbol{G} + \boldsymbol{B}_{\boldsymbol{V},\mathrm{other}}, \tag{5}$$

and $\dot{\boldsymbol{V}}_{\mathrm{Indir}}$ denotes the acceleration vector due to the indirect effect of these inputs, mediated through motion-dependent processes arising from earlier direct effects:

$$\dot{\boldsymbol{V}}_{\mathrm{Indir}} = \bar{\boldsymbol{A}}_{\boldsymbol{V},\mathrm{MDT}}(\boldsymbol{V})\boldsymbol{V} \tag{6}$$

These relationships, expressed for a continuous-time system, can be represented with a block diagram (Fig. 1).

2.2. Derivation of a recurrence formula with respect to the generalised velocity vector

The generalised acceleration vector can be expressed by difference approximation using the time interval Δt of the discrete-time system shown as:

$$\dot{\boldsymbol{V}}(k) = \frac{\boldsymbol{V}(k+1) - \boldsymbol{V}(k)}{\Delta t} \tag{7}$$

After discretising Eqs. (4) to (6), combining Eqs. (4) to (7) yields a recurrence formula for the generalised velocity vector $\boldsymbol{V}$ as follows:

$$\boldsymbol{V}(k+1) = \Delta t\dot{\boldsymbol{V}}_{\mathrm{Dir}}(k) + \boldsymbol{\Psi}_{\boldsymbol{V}}(k)\boldsymbol{V}(k), \qquad \boldsymbol{\Psi}_{\boldsymbol{V}}(k) = \boldsymbol{E}_{18} + \Delta t\bar{\boldsymbol{A}}_{\boldsymbol{V},\mathrm{MDT}}(\boldsymbol{V}(k)) \tag{8}$$

where $\boldsymbol{E}_{18}$ is the unit matrix with eighteen rows and columns.

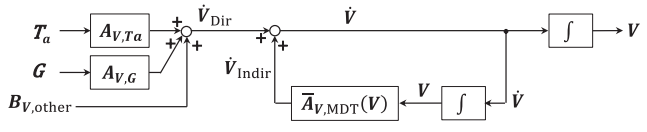

Fig. 1. A block diagram representing the relationships between accelerations arising from the direct and indirect effects of inputs (e.g. joint torques, gravity and other terms) and the generalised acceleration and velocity vectors. Plain arrows indicate multiplication of the input vector with the matrix inside the box to which the arrow is pointing, with the exception of boxes including $\int$,which correspond to a time-integral operation.

Since the coefficient matrix $\bar{\boldsymbol{A}}_{\boldsymbol{V},\mathrm{MDT}}(\boldsymbol{V}(k))$ contains the angular velocity of the generalised velocity vector $\boldsymbol{V}(k)$ in its elements, the coefficient matrix $\boldsymbol{\Psi}_{\boldsymbol{V}}(k)$ also contains the elements $\boldsymbol{V}(k)$. Although it is possible to numerically obtain the states of the individual segments (e.g. linear and angular velocity vectors) for the individual input terms using discretised Eqs.(5), (6) and (8), it would be impossible to calculate the indirect effect of the input terms using these equations because Eq. (8) is not a form of primary expression with respect to the vector $\boldsymbol{V}(k)$.

Thus, in order to quantify the indirect effect of the individual input terms, the generalised velocity vector $\boldsymbol{V}(k)$ in the matrix $\bar{\boldsymbol{A}}_{\boldsymbol{V},\mathrm{MDT}}(\boldsymbol{V}(k))$ in Eq. (8) must be replaced with the generalised velocity vector $\boldsymbol{V}(k)$ measured at the k-th time instant:

$$\begin{aligned} &\boldsymbol{V}(k+1) = \Delta t\dot{\boldsymbol{V}}_{\mathrm{Dir}}(k) + \tilde{\boldsymbol{\Psi}}_{\boldsymbol{V}}(k)\boldsymbol{V}(k), \\ &\tilde{\boldsymbol{\Psi}}_{\boldsymbol{V}}(k) = \boldsymbol{E}_{18} + \Delta t\bar{\boldsymbol{A}}_{\boldsymbol{V},\mathrm{MDT}}(\tilde{\boldsymbol{V}}(k)) \end{aligned} \tag{9}$$

Since the vector $\tilde{\boldsymbol{\Psi}}_{\boldsymbol{V}}(k)\boldsymbol{V}(k)$ has a form of primary expression with respect to the velocity vector $\boldsymbol{V}(k)$, the recurrence formula, Eq. (9), can be expressed from the beginning of the motion to the k-th time instant of analysis (Fig. 2a), and reshaped as shown in Fig. 2b, where it becomes possible to quantify the total effect (i.e. direct and indirect effects) of individual torque inputs to the generation of the generalised velocity vector.

Eqs. (5) and (9) can quantify the contributions of the individual input terms (i.e. the joint torque term, the gravitational term, the hip-joint acceleration term, the segment length fluctuation term, and the anatomical constraint joint axial angle fluctuation term) at time k to the generation of the generalised velocity vector at time $k + 1$ considering the generating factors of the MDT.

The total effects of joint torque inputs on the generation of the foot centre of gravity (CG) speed are expressed by a block diagram (Fig. 3a) consisting of the direct effect component (Fig. 3b) and indirect effect component (Fig. 3c).

The direct and indirect effects of the individual joint torque inputs in generating the MDT can be quantified from Fig. 3 (see Appendix 2 for details). The MDT contribution can be decomposed into kinematic components arising from centrifugal forces, Coriolis forces, gyroscopic effect moments and segmental length fluctuations (see Appendix 3 for details).

2.3. Data collection

Six male rugby players (two professional and four university-level; mean ± SD of age: 21.9 ± 1.8 years; height: 1.77 ± 0.06 m; body mass: 81.8 ± 4.4 kg) performed 5–8 place kicks. Each provided written informed consent, and study approval was obtained from the lead author's institution's ethics committee. The ball was placed on their preferred tee and kicked into a net approximately 4 m away. The kickers were instructed to kick as far and as straight (towards the centre of the net) as possible. Kinematic data (47 markers on the body, 6 on the ball) were recorded with a 14-camera motion capture system (VICON-MX, Vicon Motion Systems Ltd., Oxford, UK; 500 Hz). Kinetic data under the support leg were measured with a force platform (9287C, Kistler Inst.; 1000 Hz). The kicking action was divided into two phases: flight and support. These were, respectively, the period from the final take-off of the kicking foot (KFO) to ground contact with the support foot (SFC), and the period from SFC to ball contact (BC). KFO was defined as when the kicking foot's 5th MTP marker first reached a vertical displacement of 0.10 m after its final ground contact prior to ball contact (Lees and Rahnama, 2013); SFC was based on a vertical ground reaction force threshold of 10 N, and BC was defined as the frame of peak anterior toe velocity (Shinkai et al., 2009). All data were time-normalised to phase durations as −200% to −100% (flight,

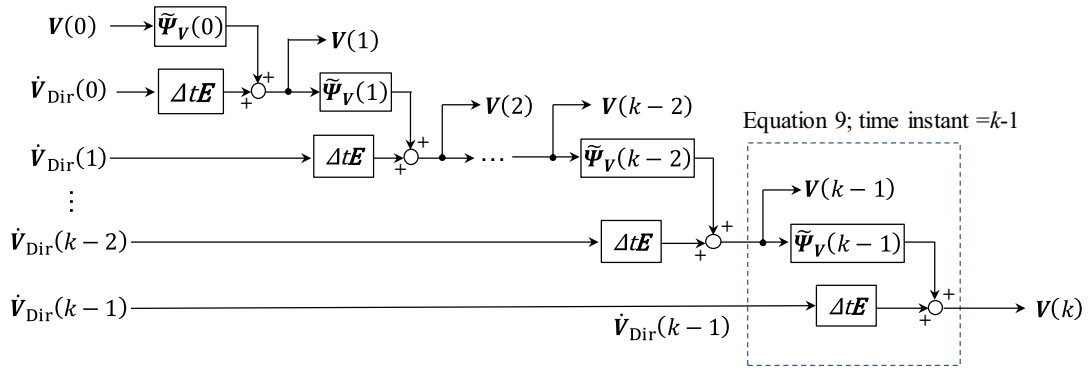

(a). A block diagram representing the recurrence formula with respect to the generalised velocity vector.

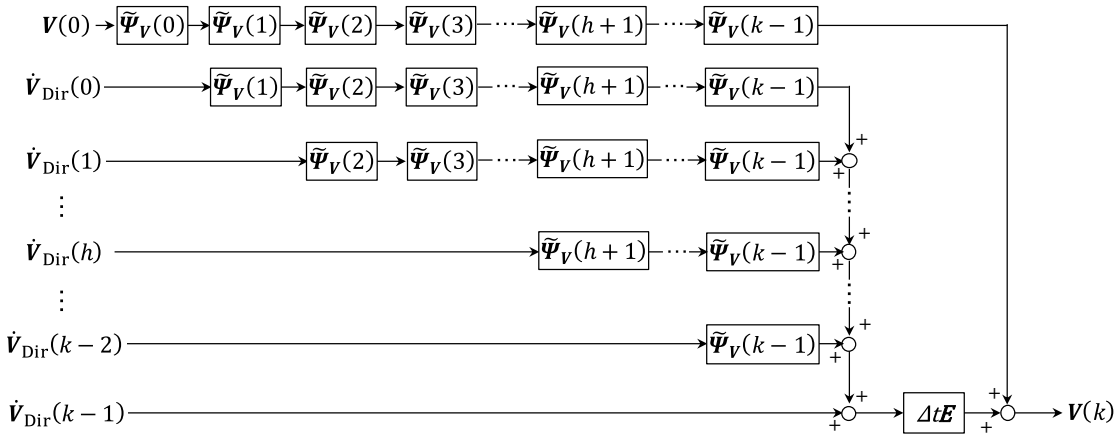

(b). A reshaped block diagram representing the recurrence formula with respect to the generalised velocity vector.

Fig. 2. A block diagram representing the recurrence formula with respect to the generalised velocity vector. Plain arrows correspond to multiplication of the input vector with the matrix inside the box to which the arrow is pointing. Reshaping Fig. 2a into b identifies the contributions due to individual terms $\dot{\boldsymbol{V}}_{\mathrm{Dir}}$, as expressed in Equation (5), at each time instant to the generation of the generalized velocity vector including the motion-dependent processes of the torque inputs arising at any later time.

KFO to SFC) and −100% to 0% (support, SFC to BC). Anatomical constraint axes (e.g. varus-valgus axis at knee joint; internal-external rotation axis at ankle joint) were also considered in the modelling (Koike et al., 2017). The coordinate data were smoothed with a fourth-order zero-phase-shift Butterworth low-pass digital filter whose optimal cut-off frequencies (5–15 Hz) were determined by residual analysis (Wells and Winter, 1980). Three trials per participant were selected based on the participants' highest subjective ratings, and the mean data across these trials were used for each participant.

3. Results

The flight and support phases lasted 0.11±0.01 and 0.13±0.01 s, respectively. The directly measured kicking foot CG speed gradually increased until −60% (normalised) time, then increased rapidly toward BC, reaching 21.34 ± 0.70 m/s at BC (Fig. 4a). The sum of the MDT and the contributions induced by the direct effect of individual terms matched the measured foot CG's speed to within 0.19 m/s throughout the movement (Fig. 4a–h). Similarly, the total of the contributions induced by both the direct and indirect effects of individual terms, following the partition of the MDT into its component indirect terms, also matched the measured foot CG's speed to within 0.14 m/s (Fig. 4a, c–h).

The MDT was the dominant contributor to the foot CG's speed. The centrifugal force component accounted for most of this MDT contribution (Fig. 4b), but the Coriolis force component was also appreciable during the support phase; the components relating to the gyroscopic effect moment and the segment length fluctuations were very small throughout. The MDT's dynamic contribution increased gradually toward −95% time, then decreased until −50%, before increasing rapidly toward BC where it reached 20.84 ± 3.67 m/s, or 98% of the foot CG's speed at this instant (Fig. 4b). After partitioning the MDT into its components, the total contribution from the direct effects of the individual joint torque inputs increased until −35% time and then decreased toward BC, while the total indirect effects of these inputs increased after −60% time toward BC (Fig. 4c). The direct effect of the initial velocity term was positive until −120% time and then became negative toward BC, whereas the indirect effect of the velocity term was positive throughout, increasing until −90% time and then decreasing toward BC (Fig. 4d). The contributions from the direct and indirect effects of the gravitational force term, the hip joint acceleration term, the segment length fluctuation term and the joint anatomical constraint axes fluctuation term were small (Fig. 4e–h).

Consideration of the time derivatives of the direct and indirect effects associated with the torques for individual joint rotations allows identification of the times when, and the specific axes about which, key contributions to the kicking foot CG's speed at BC

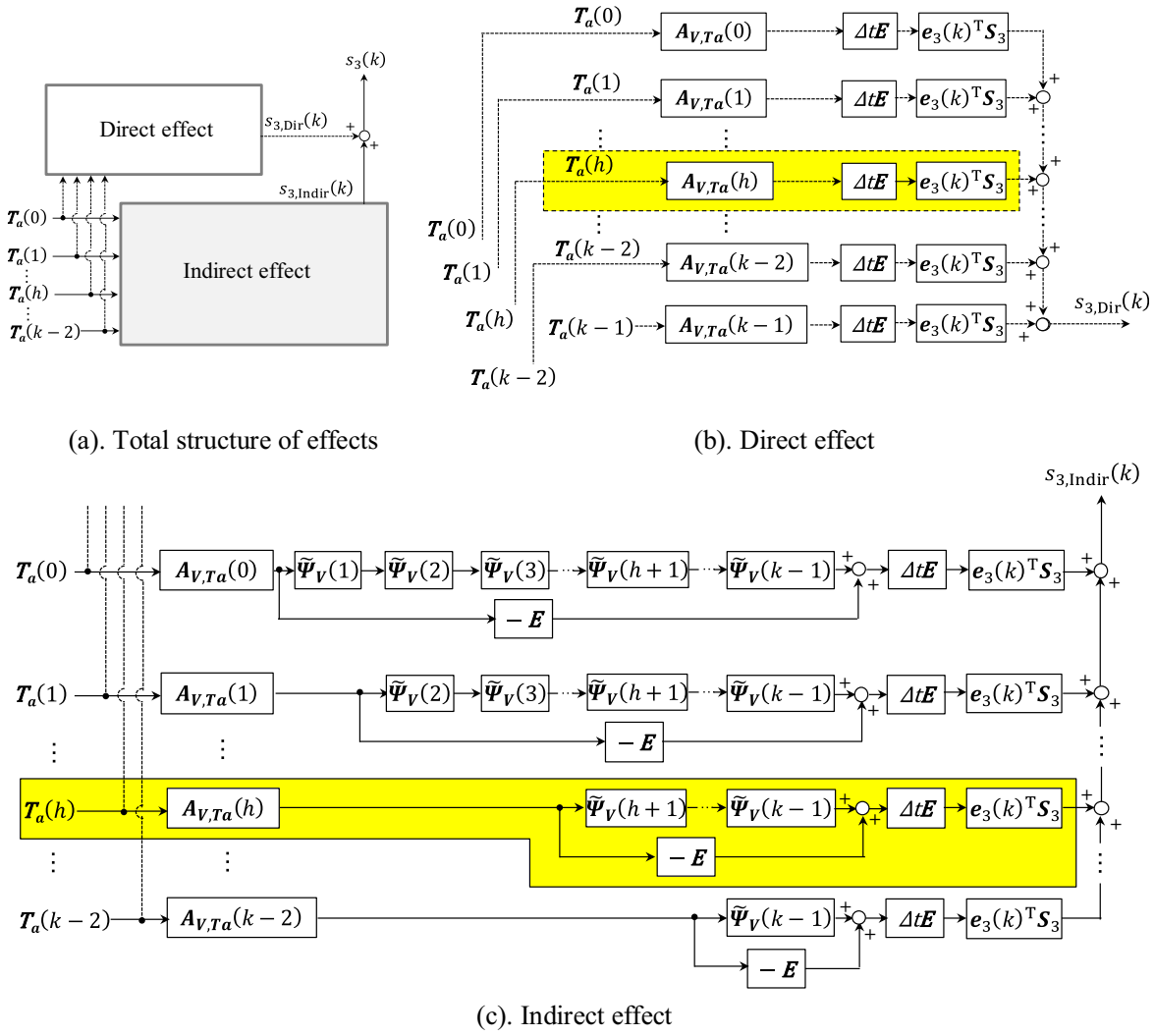

Fig. 3. A block diagram representing the direct and indirect effects of joint torque inputs to the generation of foot segment speed s_3 at time k. Plain arrows correspond to multiplication of the input vector with the matrix inside the box to which the arrow is pointing. The highlighted part of individual block diagrams in the direct effect (Fig. 3b) and the indirect effect (Fig. 3c) show respectively the contributions of the direct and indirect effects of joint torque inputs at time instant h to the generation of the foot CG's speed at BC.

($s_3(k_{BC})$; Fig. 5) occurred. Peak positive contributions from the direct and indirect effects of the hip flexion-extension torque occurred around −110 and −90% time, respectively (Fig. 5a). The indirect contributions from knee flexion-extension and ankle plantar-dorsiflexion torques were also positive (Fig. 5d and f) but these peaked slightly later (around −70% time). At this time, the direct effects of these knee and ankle torques were large and negative (Fig. 5d and f). Aside from the indirect effect of the ankle eversion-inversion torque, particularly after SFC, the other non-sagittal plane torques made only small contributions throughout the entire movement (Fig. 5b, c, e and g).

The integrated contribution across each phase to the foot CG's speed at BC was also determined for both the direct and indirect effects of each individual axial torque (Fig. 6a and b). The direct and indirect effects of the hip flexion-extension torque contributed positively to the foot CG's speed at BC across both the flight phase and the subsequent support phase. The indirect effects of the ankle plantar-dorsal flexion torques and the direct effects of the knee flexion-extension torques, both across the support phase, showed the largest positive and negative contributions, respectively.

4. Discussion

This study firstly aimed to propose and describe a method which separately quantifies the direct and indirect effects of joint torque inputs in the distal-point speed generation of a high-speed swinging motion. Secondly, we aimed to illustrate how the model outputs differ between these direct and indirect effects, using a rugby place kick as an example motion. The indirect effects of the joint torques, which are generated through motion-dependent processes as a result of previously-exerted joint torques, were the largest contributor to the foot CG's speed at BC in this rugby kicking motion (Fig. 4c). Although the overall sum of the direct effects of joint torques showed only a small contribution to the foot CG's speed at BC (Fig. 4c), the direct effect of the hip flexion-extension torque (flexor dominant throughout) was the major positive contributor to the foot CG's speed at BC, and this contributed during both flight and support (Fig. 6a and b). Interestingly, the indirect effects of the knee flexion-extension torque (extensor dominant until −20%, then flexor dominant) and ankle plantar-dorsal flexion torque (dorsiflexor dominant throughout) showed positive contributions, whereas the direct effects of those

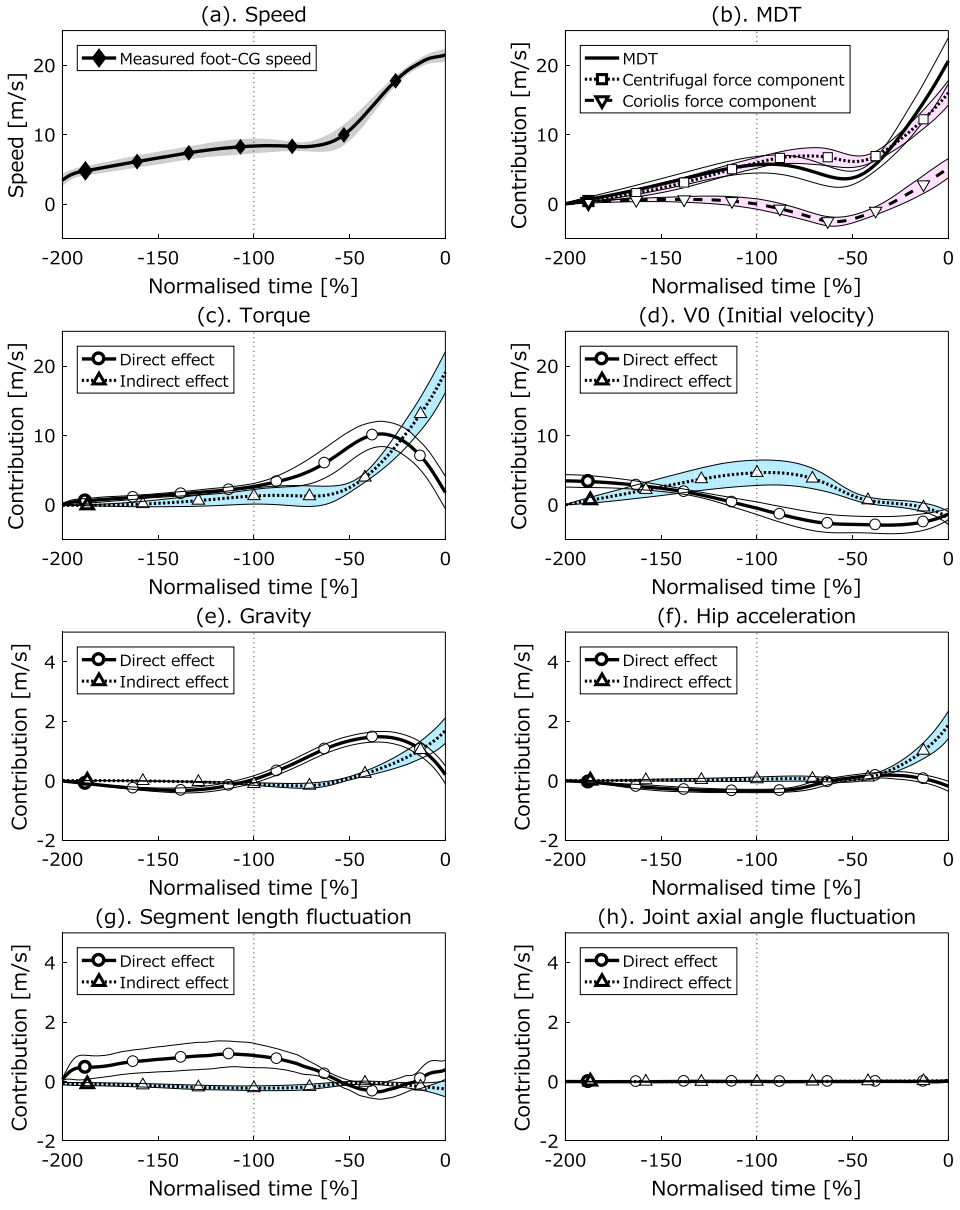

Fig. 4. Time-curve contributions of the direct and indirect effects of individual terms to the generation of the kicking foot CG's speed $s_3(k)$ for $k = -200\%$ to 0% (normalised) time. The values shown are the integrated contributions due to the direct and indirect effects of each source from $t = -200\%$ to k. Each line represents the mean across the participants at each normalised time, and the white-coloured and shaded regions indicate one standard deviation either side of the mean. Note: the scale in Figures e to h differs from the one in Figures a to d for visual purposes. For clarity, the contributions from gyroscopic effect moments and segment length fluctuations have been omitted from Figure b because the magnitudes of their mean values across the participants were less than 0.14 m/s and 0.4 m/s, respectively, throughout.

torques contributed negatively (Fig. 5d and f, Fig. 6a and b). Although exerting a knee extension torque would induce knee extension and therefore contribute geometrically to the foot CG's speed, a negative direct contribution of knee extension torque to the foot CG's speed was observed in this study. This non-intuitive phenomenon may be caused by the dynamic coupling (Kane and Levinson, 1985) of the leg segments in which the knee extension torque would induce extension of hip joint, and this hip extension would reduce the foot CG's speed, where dynamic coupling means that a torque input about one joint axis can cause multi-axial angular accelerations of the body due to the non-diagonal inertial matrix of the equation of motion for the system (Hirashima et al., 2007, 2008; Koike et al., 2017; Zajac et al., 2002, 2003). Further investigation, using an induced joint angular velocity analysis, would be needed to verify this explanation. Since a flexion torque was exerted about the hip joint throughout the movement and contributed positively to the foot CG's speed via both direct and indirect effects, torque reversal – as found to be effective in Herring and Chapman's (1992) simulation of a throwing motion – was not observed in this kicking motion. The relatively small effects of the hip joint torques about the other axes (Fig. 5b and c) support previous kinematic data which suggested that the contributions of the hip adduction-abduction and internal-external rotation angular velocities to foot speed in rugby place kicking are small (Zhang et al., 2012). Finally, the large contribution of the indirect effect of ankle plantar-dorsiflexion torques to the foot CG's speed (Fig. 5f and 6b) may be because the foot is swung with high speed around the shank and thigh segments, and therefore this torque assists in effective orientation of the foot segment. This would help to control the impact location between the foot and

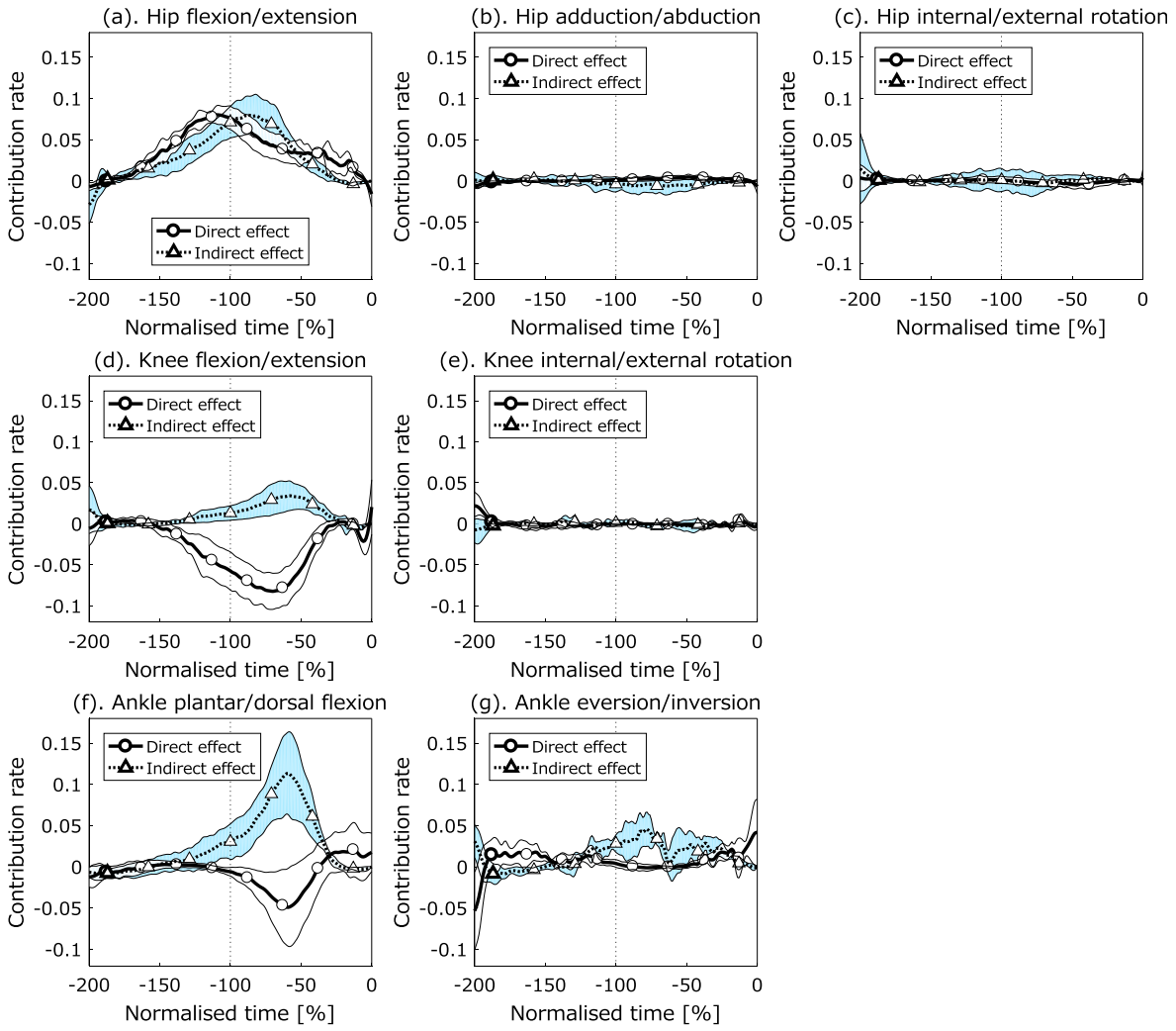

Fig. 5. Time-curve contribution rates of the direct and indirect effects of joint torque inputs at each instant during the flight and support phases to the generation of kicking-side foot CG's speed at ball contact $s_3(k_{BC})$. The units of the vertical axis for each graph are m/s per millisecond. These contribution rates indicate the time when, and the specific axis about which, each of the analysed torques induced the foot CG's speed at BC. The white-coloured and shaded regions indicate one standard deviation either side of the mean.

ball, which is an important feature for determining the ball flight characteristics (Peacock and Ball, 2017). A similar effect was also evident in the ankle eversion-inversion torque (Fig. 5g and 6b).

The method proposed in this study quantifies both the direct and indirect effects of individual joint torque inputs in the generation of distal-point speed, and their use for evaluating performance, whereas previous studies showed only the direct effect of joint torques in actions such as the generation of elbow extension angular velocity (Hirashima et al., 2008; Naito and Maruyama, 2008), of distal-point speed (Naito et al., 2017), and of angular velocities about the longitudinal axes of the upper arm and forearm segments (Naito et al., 2014) during overarm throwing and baseball pitching, and in the generation of knee extension angular velocity during a soccer kicking motion (Naito et al., 2010). Although previous studies decompose the MDT into several components in order to describe how particular kinematic features of segmental and joint movements affect the MDT contributions (e.g. Hirashima et al., 2008; Naito and Maruyama, 2008; Naito et al., 2010; Naito et al., 2017; Putnam, 1991, 1993), kinematic analyses alone cannot reveal the mechanisms by which these movements induce effective joint torques.

The capability of the algorithm to calculate the direct and indirect effects separately during the analysis of high-speed swinging motions has been demonstrated. This approach can aid in the understanding of the specific effects of individual joint torques exerted during swinging motions. For example, in rugby place kicking, high foot speed at BC is required to achieve high ball launch velocities. In our analysis of the rugby place kick, the hip flexion-extension torque exerted at around −110% time caused large foot CG speed at BC via the direct effect of the torque, and the same axial torque exerted at around −90% time induced large foot CG speed at BC via the indirect effect. Since the foot CG's speed induced solely by the direct effect of joint torques is limited by the force-producing capacity of muscles crossing the joint, utilisation of the motion-dependent mechanisms is an effective strategy for producing higher distal-point speeds during such a high-speed motion. Because the indirect effect of the hip flexion-extension torque exerted around −90% time plays a significant role in the speed generation of the foot's CG at BC by enhancing the contributions of the MDT prior to BC (Fig. 5a and 6b), it is necessary to examine the direct and indirect effects separately. The indirect effects of the knee flexion-extension and ankle plantar-dorsiflexion torques peaked after the indirect effect of the hip flexion-extension torque, and the timing of these peaks (at approximately −70% time) occurred close to where the centrifugal and Coriolis force components of the MDT inflected (Fig. 4b). While the ankle joint torque

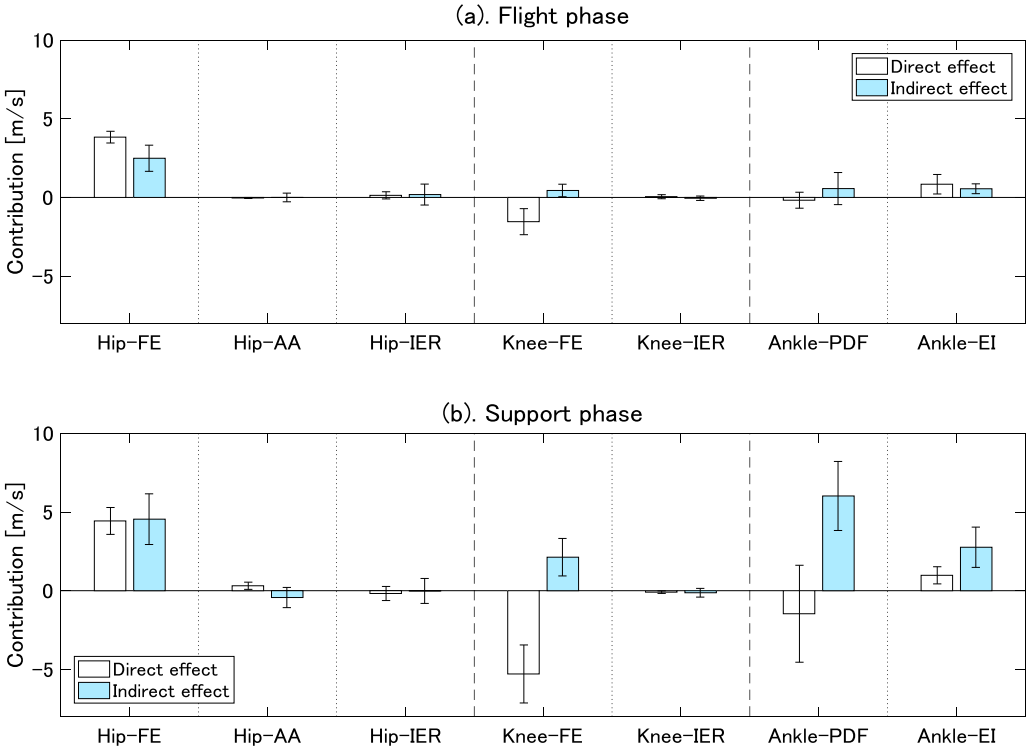

Fig. 6. Mean and standard deviation for the integrated contributions from the direct and indirect effects of joint torque inputs during the flight and support phases to the generation of foot CG's speed at ball contact; these correspond to the areas under the respective curves in Fig. 5 (pre- and post-SFC, 100%).

also plays a role via the indirect effect in the foot CG's speed generating mechanism (Fig. 5f), the role of the knee joint flexion-extension torque via the direct effect would be to prevent knee-joint hyperextension (Apriantono et al., 2006; Dörge et al., 2002) and the role of the ankle plantar-dorsiflexion torque via the direct effect may be to control the foot for accurate contact with the ball.

This study has presented the contributions to the kicking foot CG's speed using a model consisting only of the kicking-side thigh, shank and foot segments. Since the current model consists of only these segments, the contributions of joint torques other than the kicking-leg joint torques were not quantified. Thus, an analysis using a whole-body model would be necessary to fully clarify the roles of all joint torques during rugby place kicking. A more complete investigation of the whole-body kicking motion would require investigation of the contributions to the angular velocities such as joint angular velocities and foot angular velocity using a whole-body model. However, focusing on just the kicking leg is an appropriate starting point in understanding such complex high-speed swinging motions, particularly given the primary aim of our study was to detail the model and demonstrate its potential. This method can now be applied to any swinging motion, in a whole-body or part-body way, for a more complete understanding of the distal-point speed generating mechanisms. Since this approach enables the effects of joint torque inputs to be obtained even when the MDT plays a crucial role in the distal-point speed generation, estimation of muscle force contributions can be performed by solving the load distribution problem with use of musculoskeletal models (e.g. Delp et al., 2007).

5. Conclusion

A method for quantifying direct and indirect effects of joint torque inputs in the speed generating mechanism of a swinging motion has been introduced, in which a direct effect is generated by angular accelerations induced by a joint torque at a given instant, whereas an indirect effect is generated through a motion-dependent term (MDT: a nonlinear term consisting of centrifugal force, Coriolis force and gyroscopic effect moment components) induced by earlier application of a joint torque. The method allows identification of the individual joint torque axes and timings of joint torque exertion that are used to generate a high speed of the distal point of a multi-linked system. The two types of effect were quantified for joint torque inputs through a recurrence formula with respect to the generalised velocity vector of a multi-linked system based on the equation of the system's motion including a cause-and-effect relationship between joint torque inputs and motion outputs. The practical potential of this approach has been demonstrated through its application to modelling the role of the kicking-side leg in generating foot speed during a rugby place kick. Important contributions to foot CG speed, for example from the direct and indirect effects of the hip flexion-extension torque during the flight phase and the subsequent support phase, were identified by considering the factors responsible for generating the MDT. Further investigation will be needed to determine both direct and indirect effects for whole-body joint torque inputs in the generation of distal-point speed in swinging motions.

Acknowledgements

This work was partly supported by The Great Britain Sasakawa Foundation [grant numbers 5029 (Bezodis) and 5226 (Willmott)] which had no involvement in the study design, study execution, the writing of the manuscript, or the decision to submit it for publication. The authors thank Naoki Numazu for his assistance with data collection and processing.

Conflict of interest

The authors declare no conflicts of interest to report in this research.

Appendix A. Supplementary material

Supplementary material to this article can be found online at https://doi.org/10.1016/j.jbiomech.2019.01.032.

References

Apriantono, T., Nunome, H., Ikegami, Y., Sano, S., 2006. The effect of muscle fatigue on instep kicking kinetics and kinematics in association football. J. Sports Sci. 24, 951–960.

Atwater, A.E., 1979. Biomechanics of overarm throwing movements and of throwing injuries. Exerc. Sport Sci. Rev. 7, 43–85.

Delp, S.L., Anderson, F.C., Arnold, A.S., Loan, P., Habib, A., John, C.T., Thelen, D.G., 2007. OpenSim: open-source software to create and analyze dynamic simulations of movement. IEEE Trans. Biomed. Eng. 54, 1940–1950.

Dörge, H.C., Bullandersen, T., Sorensen, H., Simonsen, E.B., 2002. Biomechanical differences in soccer kicking with the preferred and the non-preferred leg. J. Sports Sci. 20, 293–299.

Elliott, B., Fleisig, G., Nicholls, R., Escamilia, R., 2003. Technique effects on upper limb loading in the tennis serve. J. Sci. Medi. Sport 6, 76–87.

Feltner, M., Dapena, J., 1986. Dynamics of the shoulder and elbow joints of the throwing arm during a baseball pitch. Int. J. Sport Biomech. 2, 235–259.

Feltner, M.E., 1989. 3-dimensional interactions in a 2-segment kinetic chain. Part II: application to the throwing arm in baseball pitching. Int. J. Sport Biomech. 5, 420–450.

Fleisig, G.S., Andrews, J.R., Dillman, C.J., Escamilla, R.F., 1995. Kinetics of baseball pitching with implications about injury mechanisms. Am. J. Sports Med. 23, 233–239.

Fleisig, G.S., Barrentine, S.W., Escamilla, R.F., Andrews, J.R., 1996a. Biomechanics of overhand throwing with implications for injuries. Sports Medicine 21, 421–437.

Fleisig, G.S., Escamilla, R.F., Andrews, J.R., Matsuo, T., Satterwhite, Y., Barrentine, S. W., 1996b. Kinematic and kinetic comparison between baseball pitching and football passing. J. Appl. Biomech. 12, 207–224.

Herring, R.M., Chapman, A.E., 1992. Effects of changes in segmental values and timing of both torque reversal in simulated throws. J. Biomech. 25, 1173–1184.

Hirashima, M., 2008. Induced acceleration analysis of three-dimensional multi-joint movements and its application to sports movements. Theoretical Biomechanics, edited Vaclav Klika, InTech.

Hirashima, M., Kudo, K., Ohtsuki, T., 2007. A new non-orthogonal decomposition method to determine effective torques for three-dimensional joint rotation. J. Biomech. 40, 871–882.

Hirashima, M., Yamane, K., Nakamura, Y., Ohtsuki, T., 2008. Kinetic chain of overarm throwing in terms of joint rotations revealed by induced acceleration analysis. J. Biomech. 41, 2874–2883.

Kane, T.R., Levinson, D.A., 1985. Dynamics: Theory and Applications. McGraw-Hill, New York, USA.

Kepple, T.M., Siegel, K.L., Stanhope, S.J., 1997. Relative contributions of the lower extremity joint moments to forward progression and support during gait. Gait Posture 6, 1–8.

Kibler, W.B., 1995. Biomechanical analysis of the shoulder during tennis activities. Clin. Sports Med. 14, 79–85.

Kindall, J., 1992. Science of coaching baseball. Human Kinetics Publishers.

Koike, S., Bezodis, N., 2017. Determining the dynamic contributions to kicking foot speed in rugby place kicking. In Proceedings of the 35th International Conference on Biomechanics in Sports, German Sport University Cologne, Cologne.

Koike, S., Harada, Y., 2014. Dynamic contribution analysis of tennis-serve-motion in consideration of torque generating mode. Procedia Eng. 72, 97–102.

Koike, S., Mimura, K., 2016a. Contributions of joint torques, motion-dependent term and gravity to the generation of baseball bat head speed. Procedia Eng. 147, 191–196.

Koike, S., Mimura, K., 2016b. Main contributors to the baseball bat head speed considering the generating factor of motion-dependent term. Procedia Eng. 147, 197–202.

Koike, S., Nakaya, S., Mori, H., Ishikawa, T., Willmott, A.P., 2017. Modelling error distribution in the ground reaction force during an induced-acceleration analysis of running in rear-foot strikers. J. Sports Sci., (Published online).

Koike, S., Uzawa, H., Hirayama, D., 2018. Generation mechanism of linear and angular ball velocity in baseball pitching. In: Proceedings 2018, 2, 206.

Lees, A., Rahnama, N., 2013. Variability and typical error in the kinematics and kinetics of the maximal instep kick in soccer. Sports Biomech. 12, 283–292.

Naito, K., Fukui, Y., Maruyama, T., 2010. Multijoint kinetic chain analysis of knee extension during the soccer instep kick. Hum. Mov. Sci. 29, 259–276.

Naito, K., Maruyama, T., 2008. Contributions of the muscular torques and motion-dependent torques to generate rapid elbow extension during overhand baseball pitching. Sports Eng. 11, 47–56.

Naito, K., Takagi, T., Kubota, H., Maruyama, T., 2017. Multi-body dynamic coupling mechanism for generating throwing arm velocity during baseball pitching. Hum. Mov. Sci. 54, 363–376.

Naito, K., Takagi, H., Yamada, N., Hashimoto, S., Maruyama, T., 2014. Intersegmental dynamics of 3D upper arm and forearm longitudinal axis rotations during baseball pitching. Hum. Mov. Sci. 38, 116–132.

Nunome, H., Asai, T., Ikegami, Y., Sakurai, S., 2002. Three-dimensional kinetic analysis of side-foot and instep soccer kicks. Med. Sci. Sports Exerc. 34, 2028–2036.

Peacock, J.C.A., Ball, K., 2017. The relationship between foot-ball impact and flight characteristics in punt kicking. Sports Eng. 20, 221–230.

Putnam, C.A., 1991. A segment interaction analysis of proximal-to-distal sequential segment motion patterns. Medi. Sci. Sports Exercise 23, 130–144.

Putnam, C.A., 1993. Sequential motions of body segments in striking and throwing skills: descriptions and explanations. J. Biomech. 26, 125–135.

Reid, M., Elliott, B., Alderson, J., 2007. Shoulder joint loading in the high performance flat and kick tennis serves. Br. J. Sports Med. 41, 884–889.

Shinkai, H., Nunome, H., Isokawa, M., Ikegami, Y., 2009. Ball impact dynamics of instep soccer kicking. Med. Sci. Sports Exerc. 41, 889–897.

Zajac, F.E., Neptune, R.R., Kautz, S.A., 2002. Biomechanics and muscle coordination of human walking. Part I: introduction to concepts, power, transfer, dynamics and simulations. Gait Posture 16, 215–232.

Zajac, F.E., Neptune, R.R., Kautz, S.A., 2003. Biomechanics and muscle coordination of human walking. Part II: lessons from dynamical simulations and clinical applications. Gait Posture 17, 1–17.

Zhang, Y., Liu, G., Xie, S., 2012. Movement sequences during instep rugby kick: a 3D biomechanical analysis. Int. J. Sports Sci. Eng. 6, 89–95.